Disulfidptosis classification of hepatocellular carcinoma reveals correlation with clinical prognosis and immune profile

tianbing wang
Anhui NO.2 Provinicial People's Hospital
Kai Guo
Anhui NO.2 Provinicial People's Hospital
Di Zhang
Hefei KingMed for Clinical Laboratory
Haibo Wang
First Affiliated Hospital of Anhui Medical University
Jimin Yin
Anhui NO.2 Provinicial People's Hospital
Haodong Cui
Anhui NO.2 Provinicial People's Hospital
Wenyong Wu (wuwenyong@ahmu.edu.cn)
Anhui NO.2 Provinicial People's Hospital

Research Article

Keywords: Hepatocellular carcinoma, Disulfidptosis, Prognosis, Immune cell infiltration, Drug sensitivity, Immunotherapy response

Posted Date: March 24th, 2023

DOI: https://doi.org/10.21203/rs.3.rs-2718172/v1

Abstract

A new mode of cell death, disulfidptosis, has been discovered. Clinical prognostic significance of disulfidptosis related pattern in hepatocellular carcinoma(HCC). In this study, a risk score model was established based on disulfidptosis model to analyze the role of risk score in clinical prognosis, immune cell infiltration, drug sensitivity and immunotherapy response. Disulfidptosis subtype were constructed based on the transcriptional profiles of 15 disulfidptosis-related genes(DRGs). All 601 samples were defined as high risk group(HRG) and low risk group(LRG) based on the disulfidptosis risk score. Drug sensitivity and response to immunotherapy were calculated by immunophenotypic score(IPS), tumor prediction, tumor immune dysfunction and rejection(TIDE). RT-qPCR was used to determine the mRNA level of disulfidptosis prognostic gene. Risk groups was identified as potential predictors of immune cell infiltration, drug sensitivity, and immunotherapy responsiveness. HRG may benefit from immunotherapy. Classification is very effective in predicting the prognosis and therapeutic effect of patients, and provides a reference for accurate individualized treatment. This study suggests that new biomarkers related to Disulfidptosis can be used in clinical diagnosis of liver cancer to predict prognosis and treatment targets.

Introduction

HCC is the most common liver tumor with the highest degree of malignancy, and its incidence is increasing year by year. HCC already ranks third among cancer deaths[1]. Among the causative factors of hepatocellular carcinoma, hepatitis B virus, hepatitis C, aflatoxin exposure and nonalcoholic steatohepatitis are the most dangerous[2]. Clinical treatment of hepatocellular carcinoma has been a problem that has plagued mankind. Despite efforts in treating hepatocellular carcinoma, recurrence and metastasis rates remain high in most patients[3]. Immune checkpoint inhibitor(ICI) therapy against PD-1/PD-L1, CTLA-4 has progressed in various cancers[4]. Nivolumab(PD1 inhibitor) has prolonged patient survival to some extent, but is effective in less than 20% of patients with hepatocellular carcinoma[5]. Therefore, there is an urgent need to understand the combination of patient stratification and biomarkers to improve hepatocellular carcinoma treatment outcomes.

Accidental cell death(ACD) and regulatory cell death(RCD) are common types of cell death[6]. Apoptosis is involved in a variety of pathophysiological processes, including tumor progression and in vivo stabilization[7]. In recent years, many emerging modalities of RCD have attracted significant attention, including: apoptosis, necroptosis, cytoplasmic division, iron death cuproptosis, autophagy-dependent cell death, immunogenic cell death, basal prolapse, lysosome-dependent cell death, endogenous cell death, reticulocyte death, etc[8, 9]. Induction of tumor cell apoptosis is the key to target cell survival or proliferation pathways, and is an important tool for tumor microenvironment therapy[10]. The inhibitory role of the death inhibitor RIPK3 in colorectal cancer has been reported, and reduced RIPK3 expression significantly reduces OS[11]. Ferroptosis has the ability to activate immune cells in tumors by delivering chemotactic signals, and iron death inducers play a role in suppressing tumor immunotherapy[12]. Recently, a study by Xiaoguang Liu et al. identified a new mode of cell death: disulfidptosis[13]. This study found that disulfidestress caused by excessive intracellular cystine accumulation can cause rapid

cell death. In glucose-deficient cancer cells with high expression of SLC7A11, the accumulation of disulfide material disrupts the normal binding of disulfide bonds between cytoskeletal proteins, resulting in the collapse of the histone skeleton and cell death. So far, the role of disulfidptosis in HCC is unclear.

In this study, we establish a risk score for disulfidptosis-related patterns to predict prognosis and guide clinical treatment. First, two disulfidptosis subtypes were identified to be associated with survival and immune infiltration. Risk scores were constructed on the basis of differentially expressed genes(DEGs) and were found to be accurate in predicting clinical prognosis, immune infiltration, tumor mutation compliance, and immunotherapy response. Our study successfully demonstrated the role of disulfidptosis patterns in HCC in prognosis prediction, immune infiltration, and immunotherapy response. It provides new ideas and methods for clinical immunotherapy planning and patient management.

Materials And Methods

Sample collection and processing

Patients' data were obtained from the TCGA(http://portal.gdc.cancer.gov/repository) and ICGC databases(https://dcc.icgc.org/). Mutation information for TCGA samples was also downloaded. The 221 HCC samples downloaded from GSE14520 in the GEO database were used as an external validation dataset. The "SVA" R software package was used to standardize the patient data from the TCGA-LIHC(371 samples) and ICGC-LIRI-JP(231 samples).

Consensus Clustering Analysis For Disulfidptosis-related Genes

15 DRGs(FLNA, FLNB, MYH9, TLN1, ACTB, MYL6, MYH10, CAPZB, DSTN, IQGAP1, ACTN4, PDLIM1, CD2AP, INF2, SLC7A11) were obtained from Liu's study[13]. The data were clustered and scored based on the expression profiles of the 15 DRGs using the "ConsensusClusterPlus" R package for consistency analysis. "Survival" R was used to analyze the survival differences between clusters. Heatmap can reflect the differences in clinical characteristics between clusters, and "pheatmap" was used to complete the analysis.

Assessment Of The Tumor Microenvironment Of Molecular Subtypes

To examine the correlation between subtypes identified by clustering and the presence of TME, imputation was used to assess all sample scores. TME scores, matrix scores, and immune scores were derived for all HCC patients using the R “ESTIMATE” procedure package. To evaluate differential immune signature in clustering, we used a single-sample gene set enrichment analysis(ssGSEA)[14]. "GSEABase" and "GSVA" were used to achieve the immune assessment. The analysis of immune-related genes between Clusters was applied to the "limma" R package, and the analysis results used "ggpubr" to draw the boxplot.

The Functional Enrichment Analysis Between Molecular Subtypes

In order to explore the potential of biological function among clusters, gene set variation analysis was performed. Function enrichment requires "c2.cp.kegg.symbol s.gmt" and "c5.go.symbol s.gmt" data from MSigDB. The "GSVA" package was used to identify genomic enrichment pathways. The criterion for statistical significance between clusters was set at an adjusted $P < 0.05$.

Identification Of Differentially Expressed Genes In Disulfidptosis Subtypes

The identification of DEGs in disulfidptosis clusters was achieved by the "limma" software package. We identified DEGs between clusters based on adjusted $P < 0.001$ and |log2FC|>1. To investigate the possible functional pathways of DEGs in each disulfidptosis cluster, the "clusterProfiler" was used to analyze the functional enrichment of GO and KEGG[15].

Establishment And Validation Of Disulfidptosis-related Prognostic Model

To quantitatively assess the relationship between disulfidptosis pattern and HCC, the disulfidptosis-related prognostic model was introduced. On the basis of cluster DEGs, Univariate Cox analysis was used to identify survival-related genes in DEGs. Subsequently, we developed a prognostic risk model for disulfidptosis using Lasso-Cox analysis. All HCC samples were defined as train set(n = 301) and test set(n = 300) according to 1:1. The disulfidptosis risk score was calculated using the model equation based on the key gene expression profiles in the model. Model Formula: Risk socre=$\sum_{i=1}^{n} expi * coefi$ (expi: gene expression, coef: gene risk factor). According to the common risk score classification rules (median method), all HCC patients participating in the study were defined as high-risk group and low-risk group. The significance of risk score in clinical prognosis was evaluated by Kaplan-Meier survival analysis. The accuracy of the model prediction is verified by Receiver-operator characteristic(ROC) curve. The constructed disulfidptosis model is also verified by the external dataset GSE14520.

Tumor Microenvironment And Immune Status In Risk Groups

The infiltration characteristics of immune cells in the tumor microenvironment(TME) were quantified using the CIBERSORT(https://cibersort.stanford.edu/about.php) algorithm for 22 immune cell species. Based on the results of the CIBERSORT algorithm, we analyzed the enrichment of immune cells in the disulfidptosis risk group. Heatmap of correlations between immune checkpoint genes and risk scores was analyzed using the "corrplot" R package. Futhermore, we quantified the differences in TME scores and immune-related gene expression between the two risk groups.

Analysis Of Tumor Mutation And Drug Sensitivity

Tumor mutation burden(TMB) generates new immunogenicity and is thought to predict immune checkpoint blockade response[16]. "maftools" R was used to map the mutation profiles of two risk groups to visualize the frequency and type of mutant genes. We used violin diagrams to visually show the differences between risk groups on TMB. The expression data and sensitivity data of targeted drugs are from genetics of drug sensitivity in cancer(GDSC)(https://www.cancerrxgene.org/) obtained. In order to analyze the difference of sensitivity between the two risk groups in different therapeutic drugs, the drug sensitivity between groups is calculated by “oncopredict” and “parallel” packages[17].

Construction And Verification Of Nomogram

We designed a nomogram based on the disulfidptosis risk score to predict the prognosis of HCC. Nomogram was constructed based on multiple clinical characteristics and risk scores of HCC patients, and the corresponding 1, 3 and 5 year survival probabilities can be queried according to the different scores of each patient. The "rms" R package is used to develop this nomogram. Calibration curves and ROC curves were used to quantify the accuracy of nomogram predictions.

Quantitative Reverse Transcription Pcr(Rt-qpcr)

According to the operation details of Tissue RNA Purification Kit Plus manual, the total tissue RNA of HCC patients was extracted. EvoM-MLVRTPremixcDNASynthesis Kit(Accurate Biotechnology, China) was used for reverse transcription of total RNA into cDNA. SYBR Green Premix Pro Taq HS qPCR Kit(AccurateBiotechnologv. China) was added during the real-time quantitative polymerase chain reaction. The sequence of primers used in the detection is shown in Supplementary Table S1.

Statistical Analyses

R version 4.2.2, GraphPad Prism 8 and SPSS25 were used for statistical analysis. Survival analysis was operated by Log-rank test. The difference analysis between groups is completed by Wilcoxon test. Spearman analysis was applied to correlation analysis. Chi-square tests or Fisher's exact tests is used for the analysis of clinical features. The set statistical difference is: $P < 0.05$.

Result

Genetic rofile of DRGs in HCC

To explore the role of DRGs in hepatocellular carcinoma, we described their genetic map. Among the 364 patients with HCC in the TCGA cohort, 26(7.14%) occurred to be regulated by disulfidptosis gene-related mutations(Fig. 1a). The mutation frequencies of FLNB and TLN1 were higher, while SLC7A11 and other

mutations did not occur in the samples. The CNV amplification frequency of 9 genes was higher than the deletion frequency, and the CNV deletion frequency of 6 genes was higher than the amplification frequency(Fig. 1b). The location of 15 DRGs on chromosomes was demonstrated in Fig. 1c. Compared to normal tissues, all DRGs except MYH10 and IQGAP1 were up-regulated in HCC(Fig. 1d). Our study also showed that the up-regulated expression of 13 DRGs suggested a poor prognosis of this HCC(Supplementary Fig. 1). There was no difference between MYH10 and IQGAP1 in survival difference. This suggests a role for DRGs in the prognosis of HCC patients.

Identification Of A Classification Pattern Of Hcc Based On The Phenotype Of Disulfidptosis

To explore the expression characteristics of DRGs in HCC, 602 study samples from the TCCA-LIHC and ICGC-LIRI-JP cohorts were clustered using a consensus clustering algorithm based on the expression data of 15DRGs. Two disulfidptosis clusters A(253 samples) and B(349 samples) were obtained by cluster analysis(Fig. 2a-c). PCA, tSNE and UAMP reduced-dimension analysis showed that the samples of An and B types were significantly clustered(Fig. 2d-f). Patients in group B had better survival in the Kaplan-Meier curve than in group A(Fig. 2g).The heatmap showed that DRGs were more abundantly expressed in subtype A than subtype B. The heatmap showed that DRGs were more abundantly expressed in subtype A than subtype B(Fig. 2h).

Tme Characteristics And Immune Infiltration Between Two Disulfidptosis Subtypes

To clarify the characteristics of the two disulfidptosis subtypes in TME, immune scores and gene expression between the two clusters were calculated in this study. In contrast to previous perceptions, cluster A was higher than cluster B in immune score, stromal score and ESTIMATE score(Fig. 3a). In addition, most immune cells were more enriched in group A than in group B(Fig. 3b-c). Among them, CD8 + Tcells, Macrophages, NK cells, Treg, APC co-inhibition, aDCs and other immunostimulatory factors were significantly expressed in patients with subtype A.This suggests that both co-stimulators and co-inhibitors may play their respective roles in cluster A. T cells in immune response are mainly activated by two signaling modes: binding of MHC to T cell receptor, co-stimulation and co-inhibition of molecular signals.Furthermore, we analyzed the expression differences of MHC-related genes, co-stimulatory/co-inhibitory factors and immune-related genes among genotypes.The expression of most HLA family genes was significantly up-regulated in cluster A(Fig. 3d). In recent years, the newly discovered expressions of MICA and MICB are also consistent. Co-stimulatory and co-repressor factors also showed expression predominance in cluster A as seen in Fig. 3e-f. Therefore, we analyze the combined effect of high immune infiltration and immunosuppression in the tumor microenvironment of HCC.

Biological Functional Analysis Of Different Disulfidptosis Subtypes

GSVA was applied to analyze the biological behavior of the two clusters. The samples of cluster A were mainly enriched in a variety of cancer-related pathways, immune system-related pathways and cytoskeleton protein-related pathways(Fig. 3g). Cluster B was enriched in biosynthesis-related pathways(Fig. 3g). To further explore the pathway relevance of the respective gene enrichment in clusters A and B, we used GSEA analysis. Highly expressed genes in cluster A were enriched in cytokine interactions and ECM receptor interactions(Fig. 3h). Low expression group genes were in concentrated in multiple amino acid metabolism and bile acid biosynthesis(Fig. 3h). Notably, the high enriched group in the B subtype was enriched in multiple amino acid metabolism, chlorophyll metabolism and bile acid biosynthesis(Fig. 3i). The low enriched group was mostly concentrated in cytokine interactions and ECM receptor interactions(Fig. 3i). Cytokines play a bidirectional role in tumors. IL-18 promotes angiogenesis, induces cancer cell proliferation and invasion, and prevents apoptosis by activating NF-κB. IL-6 similarly promotes chronic inflammatory carcinogenesis and drives intrinsic tumor progression. High doses of recombinant IL-2 were approved by the FDA in 1992 and 1998 for the treatment of metastatic renal cell carcinoma(RCC) and melanoma, respectively. The extracellular matrix(ECM) is associated with the progression of a variety of tumors including hepatocellular carcinoma, pancreatic ductal adenocarcinoma, and breast cancer. sclerosis of the ECM promotes cell proliferation, epithelial-mesenchymal transition, cancer cell metastasis, and the development of drug resistance. Sclerosis of the ECM has been reported to promote the release of tumor exosomes and activate the NORTH pathway to promote tumor invasion.The functional enrichment of these two subtypes may be responsible for the differences in patient prognosis.

Construction And Validation Of A Prognostic Model For Disulfidptosis

The classification of disulfidptosis has great potential in the clinical prognosis of hepatocellular carcinoma(HCC). In order to better understand the characteristics of disulfidptosis, we constructed a prognostic model. Initially, we identified 681 DEGs from the clusters and identified 331 prognostic-related genes through univariate Cox analysis(Supplementary Fig. 2 and Supplementary Table S2). Subsequently, Lasso-Cox regression analysis was performed on 331 prognostic genes(Fig. 4a-b), and four key genes were identified finally(Table 1). Based on these key genes, we constructed a risk score for disulfidptosis. Risk score=(-0.1806*APOC1) + (-0.2229*IL7R) + (0.0851*SPP1) + (0.2528MYBL2). We divided all HCC samples into high-risk and low-risk groups based on risk scores. The high disulfidptosis risk group had a significantly worse prognosis compared to those with a low disulfidptosis risk(Fig. 4c, $P < 0.001$). This result was confirmed by Kaplan-Meier survival curves for the test and train groups(Fig. 4d-e, $P < 0.001$). Risk curve analysis showed that increasing risk scores increased their risk of death(Fig. 4f). Risk survival analysis showed increased mortality in the high-risk group of patients, whose survival time was relatively short(Fig. 4g). In addition, we confirmed the high accuracy of the disulfide risk score in predicting prognosis after 1, 3 and 5 years. The area under the curve (AUC) values for the overall sample were 0.766, 0.736 and 0.699 for 1, 3 and 5 years(Fig. 4h). The AUC values in the internal train set were 0.808(1 year), 0.749(3 years), and 0.757(5 years)(Fig. 4i). The AUC values in the test set were 0.716, 0.704, 0.637 for 1, 3 and 5 years(Fig. 4j).

Finally, we used GSE14520 as an external independent dataset to validate the ability of the disulfidptosis risk score. We applied a risk score based on disulfidptosis to the out validation group and divided it into high and low risk groups. It has been proved that low-risk patients have a significant survival advantage(Fig. 4k). More importantly, the ROC curves showed a significant prognostic significance for the validation set cohort, with AUC values above 0.65 at 1, 3, and 5 years(Fig. 4l). Overall, our results demonstrate the good potential of the disulfidptosis risk score in evaluating prognosis.

Table 1
Multifactorial Cox regression analysis of prognosis-related DEGs.

id	coef	HR	HR.95L	HR.95H	pvalue
APOC1	-0.18059647	0.834772147	0.731772689	0.952269123	0.00719094
IL7R	-0.222889579	0.800203204	0.654681576	0.978071159	0.029519535
SPP1	0.085147213	1.088877352	1.012623953	1.170872843	0.021526195
MYBL2	0.252818907	1.287650072	1.13364786	1.462572961	0.000100197

Independent Predictive Value Of Disulfidptosis Risk Prognostic Model

We constructed a disulfidptosis risk prognostic model that demonstrated differences in survival. To further investigate, we integrated clinical information from all samples and identified three common clinical features(age, sex, stage). Our analysis showed that stage and risk score were prognostic factors for HCC(Fig. 5a and 5b). The ROC curves for risk score and stage showed their high accuracy in predicting prognosis(Fig. 5c).We also found that the risk was significantly lower in cluster B than in cluster A(Fig. 5d, $P < 0.001$). The sankey diagram illustrated that the low-risk group primarily consisted of patients belonging to subtype B, while most of the surviving patients originated from this group. Conversely, patients who passed away had higher risk scores and were predominantly from subtype A, aligning with previous analysis(Fig. 5e).

To further validate the applicability of our disulfidptosis feature model to HCC patients, we compared it with previously reported models. In the TCGA-LIHC cohort, the Tang signature[18], Wang signature[19], Zhang signature[20], and Deng signature[21] all demonstrated significant differences in survival with P values less than 0.01(Supplementary Fig. 2a-d). The AUC values for the four HCC feature models were all greater than 0.60 at 3 and 5 years(Supplementary Fig. 2e-h). Comparing the ability of the disulfidptosis feature model and the four other models to predict survival events, we found that among the C-index values of the five feature models, the disulfidptosis feature model had the highest value of 0.708, which was closer to the perfect model, followed by Tang signature(0.663), Wang signature(0.657), Deng signature(0.659), and Zhang signature(0.604)(Fig. 5f). Additionally, the RMS value of the disulfidptosis feature model was also the highest among the five models(Fig. 5g).

Disulfidptosis Risk Score Had Considerable Potential In The Prediction Of Tumor Treatment Effect

In this study, we analyzed the proportion of immune infiltration between different HCC risk groups(Supplementary Fig. 3a) and found that plasma cells were more abundantly infiltrated in the high-risk group(Fig. 6a, P = 0.006). The correlation between immune cells is shown in Supplementary Fig. 3b. Activated dendritic cells(R = 0.33, *P* = 0.018) were positively correlated with risk score(Supplementary Fig. 3c). CD8T cells, neutrophils, macrophages, activated CD4 memory cells and activated dendritic cells showed significant correlations with risk genes and scores(Supplementary Fig. 3d). Immune checkpoints are important targets for immunotherapy.The expression of CTLA4, HAVCR2, ATIC and OLA1 remained consistent with the risk score(Fig. 6b). Immunotherapy for HCC has always been a focus of attention. We also analyzed the relationship between disulfidptosis risk groups and drug treatment. The suppressive immune checkpoint genes CTLA4, HAVCR2, ATIC and OLA1 were higher in the high risk group(Fig. 6c, P < 0.01). The IPS was higher in the low risk group(Fig. 6d, P < 0.01). Low risk patients have stronger immunogenicity. In the IMvigor210 immunotherapy cohort, risk values were higher in the CR/PR(Complete Response, Partial Response) group than in the SD/PD(Progressive Disease, Stable Disease)(Fig. 6e). When comparing the proportions of patients with different immune therapy outcomes, We observed a higher proportion of CR/PR patients in the high-risk group compared to the low risk group(Fig. 6f). The lower proportion of low risk patients with high immunogenicity may be due to certain immune suppression.

Furthermore, In addition, the TIDE score assessed the clinical response to immune checkpoint inhibitor therapy. A high TIDE score indicates a low response to ICB and unfavorable tumor outcomes. TIDE score, dysfunction score were lower in the high-risk group(Fig. 6g, P < 0.001). The lower composite TIDE score obtained in the high risk group may be due to the higher proportion of immunotherapy remissions.

Analysis Of Tumor Mutations And Drug Sensitivity

Due to the increased antigenicity associated with high mutation burden, high-risk HCC tends to have a longer survival time. Tumor mutations were relatively high in high-risk groups of TCGA-LIHC(Fig. 7a, P = 0.05). Although the prognosis of the high mutation group was worse than the low mutation group(Fig. 7b), its immunotherapy effect prevailed in previous experience[22]. Subsequently, we analyzed the mutation spectrum between the high and low risk groups. The proportion of mutations observed in the 171 high risk patients was as high as 88.89%(Fig. 7c), and the mutation rate in the 190 low risk patients was 82.63%(Fig. 7d), with TP53, CTNNB1, TTN, MUC16, and PCLO genes having a high mutation frequency in both risk groups.

To identify sensitive drugs for high and low risk patients, we analyzed the sensitivity of 197 chemotherapy drugs. The sensitivity results showed that Afuresertib, KRAS(G12C), Doramapimod, Mitoxantrone, and Oxaliplatin had higher sensitivity in the high risk group(Fig. 7e-i, P < 0.001). These drugs may improve the prognosis of high risk HCC patients with disulfidptosis. Cediranib, Dasatinib,

Docetaxel, Paclitaxel, and Tozasertib had lower sensitivity in the high-risk group(Fig. 7j-n, $P < 0.001$), while the low-risk group may benefit from treatment with these drugs.

Construct A Nomogram To Predict The Survival Of Hcc

To better predict the prognosis of HCC, we constructed a nomogram for the disulfidptosis risk score. According to the constructed nomogram, each patient can obtain a 1, 3 and 5 year percentage survival coefficient according to the sum of the corresponding scores of clinical information(Fig. 8a). The 1, 3 and 5 year survival rates of the patients with a score of 236 were 0.756, 0.496 and 0.248, respectively. The cumulative hazard was higher in the high risk group(Fig. 8b). The calibration curve shows that the prediction result of the nomogram was close to the actual probability(Fig. 8c). DCA analysis shows that the nomogram and risk values have better effectiveness(Fig. 8d). The AUC values for the nomogram at 1, 3, and 5 years are 0.762, 0.743, and 0.702, respectively(Fig. 8e). The AUC values of the internal train set are all greater than 0.75(0.804 for 1 year, 0.760 for 3 years, and 0.763 for 5 years, Supplementary Fig. 4a). The internal test set confirms the high accuracy of the overall survival for 1, 3, and 5 years of the nomogram(Supplementary Fig. 4b). Additionally, in the external validation set GSE14520, the AUC values for the nomogram predicting 1, 3, and 5 years are all greater than 0.6(Supplementary Fig. 4c). The calibration curve shows that the internal train set, test set, and external validation set are all very close to the actual accuracy values (Supplementary Fig. 4d-f). All of these indicate that the disulfidptosis-related nomogram has high value in predicting the survival time of HCC patients.

Spp1 And Mybl2 Can Predict The Prognosis Of Hcc

We also analyzed the ability of four genes to predict the prognosis of HCC. The AUC of ROC curve was APOC1(0.425), SPP1(0.651), IL7R(0.487) and MYBL2(0.636), respectively(Fig. 8f). It can be seen that SPP1 and MYBL2 play an important role in predicting the prognosis of HCC. Based on the four biomarkers in the disulfidptosis model, we explored their ability in HCC. First of all, we collected 10 pairs of HCC and corresponding adjacent normal tissues for local tissue verification, extracted and collected RNA from the tissues for reverse transcription, and then used cDNA for qPCR experiment. The results of PCR showed that the mRNA content of APOC1, SPP1 and MYBL2 in HCC tissues was higher than that in paracancerous tissues(Fig. 8g-i). The mRNA level of IL7R is relatively low in HCC organizations(Fig. 8j). The protein immunohistochemical staining results of APOC1, SPP1 and MYBL2 were obtained from the HPA. It can be seen from Fig. 8k that APOC1, SPP1 and MYBL2 are moderately or highly stained in HCC tissues and weakly stained in normal liver tissues. This is consistent with the level of mRNA.

Discussion

As a common malignant tumor, hepatocellular carcinoma is usually asymptomatic and rapidly progressive, and the prognosis of patients is generally poor. Patients with early stage hepatocellular carcinoma are usually treated with traditional therapies: surgical resection, radiofrequency ablation,

TACE[23–25]. Liver transplantation is recognized as the most effective radical treatment for hepatocellular carcinoma, but it is not yet widely available due to lack of liver resources. For patients with advanced disease, only palliative treatment is available. In recent years, with the rise of immunotherapy, treatment options for patients with advanced hepatocellular carcinoma have advanced significantly. Many studies have shown that the prognosis and treatment response of patients with hepatocellular carcinoma are closely related to the immune cell component[26–31].

As a new mode of cell death, the role of disulfidptosis in tumorigenesis is unclear. Disulfide plays a recurrent role in cancer. Reports have shown that the polymerization of disulfide bonds in mitochondria can alter tumor progression[32]. A disulfide molybdenum disulfide(MoS2) can target cancer treatment diagnostics when combined with a metal organic skeleton[33]. Xiaoguang Liu et al proposed that the accumulation of disulfide in tumor cells leads to cell disintegration and death, which provides a new direction for the treatment of tumors[13].

The current classification methods regarding HCC are mainly based on the pathological characteristics of cancer cells. With many studies, HCC subtypes based on different features can also reveal clinical relevance and prognostic value[34, 35]. Our study classified patients into 2 disulfidptosis subtypes based on unsupervised clustering in an attempt to provide a role for discovering new feature patterns in HCC for tumor progression and treatment.

It is found that the change of their expression can lead to differences in prognosis(except MYH10 and IQGAP1). 13 highly expressed DRGs bring poor prognosis in patients with HCC. The expression of DRGs with increased copy number in HCC is up-regulated, indicating that copy number amplification can promote the overexpression of the gene. In the 602 samples we included in the study, combined with prognosis, we found that high disulfidptosis subtypes predicted a poor prognosis.

Low disulfidptosis subtype can bring better prognosis to patients. The degradation and death of redox system of cancer cells can be saved by the accumulation of disulfide bonds in tissues and cells[36]. This reveals the key pathway of disulfidptosis as an anti-tumor cell. We also found the immune infiltration of disulfidptosis subtypes in TME. It is worth noting that the high disulfidptosis subtypes had higher immune cells and immune scores. This is different from previous perceptions. After analyzing the stimulation mode of immune activation pathway, it was found that there was not only high expression of CD274, ICOS and other costimulatory factors in high isulfidptosis subtypes, but also up-regulated expression of co-suppressors such as CTLA4, BTLA, LAG3 and TIGIT. Co-signaling pathway targeting T cells has become the main category of immunotherapy[37]. In general, the high degree of infiltration of CD8 + T cells often indicates a better survival prognosis. However, there was more CD8 + T cell infiltration in the high disulfidptosis subtype with poor prognosis. A study of melanoma found that upregulation of CD8 + T cells was associated with shorter overall survival[28]. Colorectal cancer-related studies suggest that hyperosmosis of CD8 + T cells leads to up-regulation of FOXP3 and down-regulation of E-cadherin, resulting in a poor prognosis[38]. The infiltration of CD8 + T cells may lead to further mutation and evolution of tumor cells, thus increasing their ability of immune escape. In non-small cell lung cancer,

high content of CD8 + T cells is consistent with tumor cell mutation load and genomic instability[39]. CD8 + T cell infiltration is an important index of tumor immune surveillance. High level of CD8 + T cell infiltration may lead to tumor immune escape and deterioration of prognosis.

In order to explore the role of disulfidptosis features in HCC, we screened four key genes from DEGs between subtypes: APOC1, IL7R, SPP1 and MYBL2. A prognostic risk model is constructed based on four genetic characteristics, and its accuracy is verified internally and externally. Disulfidptosis characteristic model plays an important role in independently predicting prognosis, tumor immune infiltration and tumor mutation load. Compared with regular stage, disulfidptosis characteristic risk score is more prominent in predicting prognosis. In the previous study, Tang, Wang, Zhang and and Deng constructed four HCC prognostic models and verified them. Compared with their model, the disulfidptosis characteristic model in this study has the best ability in predicting prognosis. This confirms the direction of our research. Subsequently, we discussed the role of high and low risk in immunotherapy response. Four immunosuppressive checkpoints, CTLA4, HAVCR2, ATIC and and OLA1, were upregulated in the high disulfidptosis risk group, which may explain their poor prognosis. IPS obtains immune checkpoints from the TCIA database(https://tcia.at/), and is often used as a reference indicator of the degree of benefit of immune checkpoint inhibitors[40]. The low disulfidptosis risk group showed higher IPS, and the immune checkpoint effect may be better. In the analysis of the results of immunotherapy for metastatic bladder cancer, it was found that the proportion of remission patients in the low disulfidptosis risk group was lower[41]. The different result may be the immunosuppression of the tumor. The results of the TIDE score confirmed our conjecture that there was a higher immunosuppression score in the low disulfidptosis risk group. This explains why the high disulfidptosis risk group benefits from immunotherapy. TIDE is more accurate and effective than other indicators in predicting the prognosis of melanoma patients receiving anti-PD1 or CTLA4 therapy[42]. Immune dysfunction score and rejection score are used to guide clinical medication and improve the accuracy of treatment.

There is a certain correlation between TMB and tumor prognosis and survival. Some clinical trials have shown that tumor patients with high TMB have a better prognosis when receiving immunotherapy.For example, a study of patients with NSCLC found that patients with high TMB had longer overall survival when treated with PD-1/PD-L1 antibodies[43]. There are similar results in colorectal cancer[44]. In our study, patients with high disulfidptosis risk scores had more TMB and were likely to have a longer survival period. Patients with high risk of disulfidptosis were more sensitive to Afuresertib, KRAS(G12C), Doramapimod, Mitoxantrone and and Oxaliplatin. As a new inhibitor of AKT signal pathway, Afuresertib can be used to treat a variety of tumors. Studies in esophageal cancer have found that Afuresertib antagonizes tumor progression mainly by inhibiting the expression of PI3K and Akt pathway proteins[45]. Ceritinib can increase the sensitivity of Afuresertib in gastric cancer and lead to the increase of tumor cell apoptosis[46]. Afuresertib can also significantly proliferate malignant pleural mesothelioma cells[47]. Colon cancer patients with KRAS(G12C) mutations can benefit from treatment with KRAS(G12C) inhibitors[48]. Doramapimod is a p38 MAPK inhibitor, which can inhibit the proliferation of NSCLC by activating p38-MAPK pathway[49]. Oxaliplatin interferes with DNA synthesis and repair by binding to DNA, thus inhibiting the proliferation and spread of tumor cells[50]. In recent years, Oxaliplatin has been

frequently used in gastrointestinal tumors and achieved good results[50]. These drugs have a significant inhibitory effect on tumor cells and are undoubtedly a good choice for high disulfidptosis risk.

Finally, this study studies the key genes of disulfidptosis characteristics, and SPP1 and MYBL2 have excellent ability to predict the survival of HCC patients. SPP1(secretory phosphoprotein 1) is an acidic glycoprotein expressed in many cell types. Its role in tumor has been widely studied[51–53]. SPP1 is involved in the proliferation, migration, invasion and metastasis of tumor cells. Overexpression of SPP1 maintained the activation of P13K/AKT pathway in prostate cancer, while low expression inhibited the invasion and migration of tumor cells[54]. The overexpression of SPP1 in melanoma is associated with poor prognosis of melanoma[55]. SPP1 also plays a role in the regulation of immune process. SPP1 regulates the immune system of mice by up-regulating IL-12 and IFN γ[56]. The role and mechanism of SPP1 in HCC has not been elucidated. Our study found that it is highly expressed in HCC and may also play the role of oncogenes. It has been reported that MYBL2, as a transcription factor, plays a role in tumors. MYBL2 can regulate cell proliferation and differentiation and participate in the process of cell cycle. MYBL2 promotes the proliferation and metastasis of bladder cancer cells through high expression[57]. ABRACL is regulated by MYBL2 transcription factors and promotes the malignant progression of breast cancer cells[58]. OPA3 is highly expressed in HCC and participates in tumor cell proliferation and aerobic glycolysis. MYBL2 can regulate OPA3 to increase its effect[59]. Our study also shows that the expression of transcription factor MYBL2 in HCC is up-regulated, which may lead to poor prognosis by enhancing the expression of oncogenes. In order to make the disulfidptosis model more practical in clinic, we created the nomogram diagram. It can directly reflect the survival probability of each patient.

However, our research also has some limitations. First of all, our research needs more independent queues and larger sample size to verify the accuracy of the model, although this study has used some independent queues for verification. Our research is a retrospective study of HCC, and we need to continue to improve the basic experiments to verify the function and mechanism of genes, which will be the direction of our future efforts.

Overall, our study is the first to combine the disulfidptosis subtype pattern with immune infiltration in patients with hepatocellular carcinoma. The cluster identification helps to understand the immune infiltration of patients at different levels. We quantitatively constructed the disulfidptosis risk score, which has an accurate predictive role in prognostic assessment of tumor patients, immunotherapy response, and is a new biomarker for prognosis and treatment. This study also identified key prognostic genes associated with hepatocarcinogenesis and validated their expression in HCC, providing new targets and directions for the prognosis and treatment of hepatocellular carcinoma. In summary, this study provides a new quantitative scoring method for clinicians to develop accurate and personalized treatment plans, which is equally applicable to prognosis prediction and immunotherapy prediction

Declarations

Data availability statement Publicly available datasets were used in this study. This data can be found here: TCGA database (http://portal.gdc.cancer.gov/repository), ICGC database(https://dcc.icgc.org/), GEO database(GSE14520) (http://www.ncbi.nlm.nih.gov/geo/), IMvigor210 cohort (http://research-pub.gene.com/IMvigor210CoreBiologies/), CIBERSORT (https://cibersort.stanford.edu/about.php), TCIA database (https://tcia.at/), GDSC database (https://www.cancerrxgene.org/), TIDE database (http://tide.dfci.harvard.edu), HPA database(http://www.proteinatlas.org).

Acknowledgements All the authors would like to thank the specimen donors and the information from TCGA, ICGC and GSE14520 databases used in this study.

Author contributions TBW provided the design concept of this study, TBW and DZ drafted the manuscript, TBW, DZ, KG, HBW, JMY,HDC and WYW collected, processed and analyzed the data, and TBW, KG, HBW, JMY, HDC and DZ completed the drawing of the numbers and the revision of the manuscript. All authors contributed to this article and read and approved the final manuscript. All authors had full access to all of the data in the study and had final responsibility for the decision to submit for publication.

Funding This work was supported by the research and development of key common technologies and engineering projects of major scientific and technological achievements in Hefei, China [number 2021YL001] and the key research and development program special program on population health in Anhui Province, China [number 202104j07020005] under Grant. The datasets generated and/or analyzed during the current study are available from the corresponding author on reasonable request. All authors have responsibility for the decision to submit for publication and declare no competing interests.

Conflct of interest The authors declare no competing interests.

Ethical approval The research scheme was approved by the Clinical Medical Ethics Committee of the First Affiliated Hospital of Anhui Medical University(Approved ID: PJ2022-07-65), which conforms to the provisions of the Helsinki Declaration. The authors consent for publication.

References

1. Sung H, Ferlay J, Siegel RL, Laversanne M, Soerjomataram I, Jemal A et al (2021) Global Cancer Statistics 2020: GLOBOCAN Estimates of Incidence and Mortality Worldwide for 36 Cancers in 185 Countries. Ca Cancer J Clin 71(3):209-249. https://10.3322/caac.21660
2. Llovet JM, Zucman-Rossi J, Pikarsky E, Sangro B, Schwartz M, Sherman M et al (2016) Hepatocellular carcinoma. Nat Rev Dis Primers 2:16018. https://10.1038/nrdp.2016.18
3. Stravitz RT, Heuman DM, Chand N, Sterling RK, Shiffman ML, Luketic VA et al (2008) Surveillance for hepatocellular carcinoma in patients with cirrhosis improves outcome. Am J Med 121(2):119-126. https://10.1016/j.amjmed.2007.09.020
4. Hoos A (2016) Development of immuno-oncology drugs — from CTLA4 to PD1 to the next generations. Nat Rev Drug Discov 15(4):235-247. https://10.1038/nrd.2015.35

5. El-Khoueiry AB, Sangro B, Yau T, Crocenzi TS, Kudo M, Hsu C et al (2017) Nivolumab in patients with advanced hepatocellular carcinoma (CheckMate 040): an open-label, non-comparative, phase 1/2 dose escalation and expansion trial. Lancet 389(10088):2492-2502. https://10.1016/S0140-6736(17)31046-2
6. Kerr JF, Wyllie AH, Currie AR (1972) Apoptosis: a basic biological phenomenon with wide-ranging implications in tissue kinetics. Br J Cancer 26(4):239-257. https://10.1038/bjc.1972.33
7. Koren E, Fuchs Y (2021) Modes of Regulated Cell Death in Cancer. Cancer Discov 11(2):245-265. https://10.1158/2159-8290.CD-20-0789
8. Galluzzi L, Vitale I, Aaronson SA, Abrams JM, Adam D, Agostinis P et al (2018) Molecular mechanisms of cell death: recommendations of the Nomenclature Committee on Cell Death 2018. Cell Death Differ 25(3):486-541. https://10.1038/s41418-017-0012-4
9. Tang D, Kang R, Berghe TV, Vandenabeele P, Kroemer G (2019) The molecular machinery of regulated cell death. Cell Res 29(5):347-364. https://10.1038/s41422-019-0164-5
10. Carneiro BA, El-Deiry WS (2020) Targeting apoptosis in cancer therapy. Nat Rev Clin Oncol 17(7):395-417. https://10.1038/s41571-020-0341-y
11. Feng X, Song Q, Yu A, Tang H, Peng Z, Wang X (2015) Receptor-interacting protein kinase 3 is a predictor of survival and plays a tumor suppressive role in colorectal cancer. Neoplasma 62(4):592-601. https://10.4149/neo_2015_071
12. Garg AD, Agostinis P (2017) Cell death and immunity in cancer: From danger signals to mimicry of pathogen defense responses. Immunol Rev 280(1):126-148. https://10.1111/imr.12574
13. Liu X, Nie L, Zhang Y, Yan Y, Wang C, Colic M et al (2023) Actin cytoskeleton vulnerability to disulfide stress mediates disulfidptosis. Nat Cell Biol 25(3):404-414. https://10.1038/s41556-023-01091-2
14. Subramanian A, Tamayo P, Mootha VK, Mukherjee S, Ebert BL, Gillette MA et al (2005) Gene set enrichment analysis: a knowledge-based approach for interpreting genome-wide expression profiles. Proc Natl Acad Sci U S a 102(43):15545-15550. https://10.1073/pnas.0506580102
15. Yu G, Wang LG, Han Y, He QY (2012) clusterProfiler: an R package for comparing biological themes among gene clusters. Omics 16(5):284-287. https://10.1089/omi.2011.0118
16. Chan TA, Yarchoan M, Jaffee E, Swanton C, Quezada SA, Stenzinger A et al (2019) Development of tumor mutation burden as an immunotherapy biomarker: utility for the oncology clinic. Ann Oncol 30(1):44-56. https://10.1093/annonc/mdy495
17. Maeser D, Gruener RF, Huang RS (2021) oncoPredict: an R package for predicting in vivo or cancer patient drug response and biomarkers from cell line screening data. Brief Bioinform 22(6). https://10.1093/bib/bbab260
18. Tang Y, Xu L, Ren Y, Li Y, Yuan F, Cao M et al (2022) Identification and Validation of a Prognostic Model Based on Three MVI-Related Genes in Hepatocellular Carcinoma. Int J Biol Sci 18(1):261-275. https://10.7150/ijbs.66536
19. Wang Z, Pan L, Guo D, Luo X, Tang J, Yang W et al (2021) A novel five-gene signature predicts overall survival of patients with hepatocellular carcinoma. Cancer Med 10(11):3808-3821.

https://10.1002/cam4.3900

20. Zhang Z, Zeng X, Wu Y, Liu Y, Zhang X, Song Z (2022) Cuproptosis-Related Risk Score Predicts Prognosis and Characterizes the Tumor Microenvironment in Hepatocellular Carcinoma. Front Immunol 13:925618. https://10.3389/fimmu.2022.925618
21. Deng T, Hu B, Jin C, Tong Y, Zhao J, Shi Z et al (2021) A novel ferroptosis phenotype-related clinical-molecular prognostic signature for hepatocellular carcinoma. J Cell Mol Med 25(14):6618-6633. https://10.1111/jcmm.16666
22. Snyder A, Makarov V, Merghoub T, Yuan J, Zaretsky JM, Desrichard A et al (2014) Genetic basis for clinical response to CTLA-4 blockade in melanoma. N Engl J Med 371(23):2189-2199. https://10.1056/NEJMoa1406498
23. Vitale A, Peck-Radosavljevic M, Giannini EG, Vibert E, Sieghart W, Van Poucke S et al (2017) Personalized treatment of patients with very early hepatocellular carcinoma. J Hepatol 66(2):412-423. https://10.1016/j.jhep.2016.09.012
24. Forner A, Reig M, Bruix J (2018) Hepatocellular carcinoma. Lancet 391(10127):1301-1314. https://10.1016/S0140-6736(18)30010-2
25. Clavien PA, Lesurtel M, Bossuyt PM, Gores GJ, Langer B, Perrier A (2012) Recommendations for liver transplantation for hepatocellular carcinoma: an international consensus conference report. Lancet Oncol 13(1):e11-e22. https://10.1016/S1470-2045(11)70175-9
26. Cheng AL, Hsu C, Chan SL, Choo SP, Kudo M (2020) Challenges of combination therapy with immune checkpoint inhibitors for hepatocellular carcinoma. J Hepatol 72(2):307-319. https://10.1016/j.jhep.2019.09.025
27. Kurebayashi Y, Ojima H, Tsujikawa H, Kubota N, Maehara J, Abe Y et al (2018) Landscape of immune microenvironment in hepatocellular carcinoma and its additional impact on histological and molecular classification. Hepatology 68(3):1025-1041. https://10.1002/hep.29904
28. Tumeh PC, Harview CL, Yearley JH, Shintaku IP, Taylor EJ, Robert L et al (2014) PD-1 blockade induces responses by inhibiting adaptive immune resistance. Nature 515(7528):568-571. https://10.1038/nature13954
29. Fridman WH, Zitvogel L, Sautes-Fridman C, Kroemer G (2017) The immune contexture in cancer prognosis and treatment. Nat Rev Clin Oncol 14(12):717-734. https://10.1038/nrclinonc.2017.101
30. Thorsson V, Gibbs DL, Brown SD, Wolf D, Bortone DS, Ou YT et al (2018) The Immune Landscape of Cancer. Immunity 48(4):812-830. https://10.1016/j.immuni.2018.03.023
31. Riaz N, Havel JJ, Makarov V, Desrichard A, Urba WJ, Sims JS et al (2017) Tumor and Microenvironment Evolution during Immunotherapy with Nivolumab. Cell 171(4):934-949. https://10.1016/j.cell.2017.09.028
32. Kim S, Jana B, Go EM, Lee JE, Jin S, An EK et al (2021) Intramitochondrial Disulfide Polymerization Controls Cancer Cell Fate. Acs Nano 15(9):14492-14508. https://10.1021/acsnano.1c04015
33. Yang S, Li D, Chen L, Zhou X, Fu L, You Y et al (2021) Coupling metal organic frameworks with molybdenum disulfide nanoflakes for targeted cancer theranostics. Biomater Sci 9(9):3306-3318.

https://10.1039/d0bm02012e

34. Wang Y, Zhang Y, Wang L, Zhang N, Xu W, Zhou J et al (2022) Development and experimental verification of a prognosis model for cuproptosis-related subtypes in HCC. Hepatol Int 16(6):1435-1447. https://10.1007/s12072-022-10381-0
35. He Q, Yang J, Jin Y (2022) Immune infiltration and clinical significance analyses of the coagulation-related genes in hepatocellular carcinoma. Brief Bioinform 23(4). https://10.1093/bib/bbac291
36. Liu X, Olszewski K, Zhang Y, Lim EW, Shi J, Zhang X et al (2020) Cystine transporter regulation of pentose phosphate pathway dependency and disulfide stress exposes a targetable metabolic vulnerability in cancer. Nat Cell Biol 22(4):476-486. https://10.1038/s41556-020-0496-x
37. Chen L, Flies DB (2013) Molecular mechanisms of T cell co-stimulation and co-inhibition. Nat Rev Immunol 13(4):227-242. https://10.1038/nri3405
38. Galon J, Costes A, Sanchez-Cabo F, Kirilovsky A, Mlecnik B, Lagorce-Pages C et al (2006) Type, density, and location of immune cells within human colorectal tumors predict clinical outcome. Science 313(5795):1960-1964. https://10.1126/science.1129139
39. Kadara H, Choi M, Zhang J, Parra ER, Rodriguez-Canales J, Gaffney SG et al (2017) Whole-exome sequencing and immune profiling of early-stage lung adenocarcinoma with fully annotated clinical follow-up. Ann Oncol 28(1):75-82. https://10.1093/annonc/mdw436
40. Liu X, Wu S, Yang Y, Zhao M, Zhu G, Hou Z (2017) The prognostic landscape of tumor-infiltrating immune cell and immunomodulators in lung cancer. Biomed Pharmacother 95:55-61. https://10.1016/j.biopha.2017.08.003
41. Necchi A, Joseph RW, Loriot Y, Hoffman-Censits J, Perez-Gracia JL, Petrylak DP et al (2017) Atezolizumab in platinum-treated locally advanced or metastatic urothelial carcinoma: post-progression outcomes from the phase II IMvigor210 study. Ann Oncol 28(12):3044-3050. https://10.1093/annonc/mdx518
42. Jiang P, Gu S, Pan D, Fu J, Sahu A, Hu X et al (2018) Signatures of T cell dysfunction and exclusion predict cancer immunotherapy response. Nat Med 24(10):1550-1558. https://10.1038/s41591-018-0136-1
43. Rizvi NA, Hellmann MD, Snyder A, Kvistborg P, Makarov V, Havel JJ et al (2015) Cancer immunology. Mutational landscape determines sensitivity to PD-1 blockade in non-small cell lung cancer. Science 348(6230):124-128. https://10.1126/science.aaa1348
44. Schrock AB, Ouyang C, Sandhu J, Sokol E, Jin D, Ross JS et al (2019) Tumor mutational burden is predictive of response to immune checkpoint inhibitors in MSI-high metastatic colorectal cancer. Ann Oncol 30(7):1096-1103. https://10.1093/annonc/mdz134
45. Min B, Wang Y, Liang F, Wang CX, Wang F, Yang Z (2022) The Protective Mechanism of Afuresertib against Esophageal Cancer. Dis Markers 2022:1832241. https://10.1155/2022/1832241
46. Wang J, Xu X, Wang T, Guo Q, Dai X, Guo H et al (2021) Ceritinib increases sensitivity of AKT inhibitors to gastric cancer. Eur J Pharmacol 896:173879. https://10.1016/j.ejphar.2021.173879

47. Yamaji M, Ota A, Wahiduzzaman M, Karnan S, Hyodo T, Konishi H et al (2017) Novel ATP-competitive Akt inhibitor afuresertib suppresses the proliferation of malignant pleural mesothelioma cells. Cancer Med 6(11):2646-2659. https://10.1002/cam4.1179
48. Amodio V, Yaeger R, Arcella P, Cancelliere C, Lamba S, Lorenzato A et al (2020) EGFR Blockade Reverts Resistance to KRAS(G12C) Inhibition in Colorectal Cancer. Cancer Discov 10(8):1129-1139. https://10.1158/2159-8290.CD-20-0187
49. Wang J, Li J, Cao N, Li Z, Han J, Li L (2018) Resveratrol, an activator of SIRT1, induces protective autophagy in non-small-cell lung cancer via inhibiting Akt/mTOR and activating p38-MAPK. Onco Targets Ther 11:7777-7786. https://10.2147/OTT.S159095
50. Zhang C, Xu C, Gao X, Yao Q (2022) Platinum-based drugs for cancer therapy and anti-tumor strategies. Theranostics 12(5):2115-2132. https://10.7150/thno.69424
51. Dalla-Torre CA, Yoshimoto M, Lee CH, Joshua AM, de Toledo SR, Petrilli AS et al (2006) Effects of THBS3, SPARC and SPP1 expression on biological behavior and survival in patients with osteosarcoma. Bmc Cancer 6:237. https://10.1186/1471-2407-6-237
52. Anborgh PH, Caria LB, Chambers AF, Tuck AB, Stitt LW, Brackstone M (2015) Role of plasma osteopontin as a biomarker in locally advanced breast cancer. Am J Transl Res 7(4):723-732.
53. Sharon Y, Raz Y, Cohen N, Ben-Shmuel A, Schwartz H, Geiger T et al (2015) Tumor-derived osteopontin reprograms normal mammary fibroblasts to promote inflammation and tumor growth in breast cancer. Cancer Res 75(6):963-973. https://10.1158/0008-5472.CAN-14-1990
54. Pang X, Zhang J, He X, Gu Y, Qian BZ, Xie R et al (2021) SPP1 Promotes Enzalutamide Resistance and Epithelial-Mesenchymal-Transition Activation in Castration-Resistant Prostate Cancer via PI3K/AKT and ERK1/2 Pathways. Oxid Med Cell Longev 2021:5806602. https://10.1155/2021/5806602
55. Deng G, Zeng F, Su J, Zhao S, Hu R, Zhu W et al (2020) BET inhibitor suppresses melanoma progression via the noncanonical NF-kappaB/SPP1 pathway. Theranostics 10(25):11428-11443. https://10.7150/thno.47432
56. Rabinowich H, Lin WC, Amoscato A, Herberman RB, Whiteside TL (1995) Expression of vitronectin receptor on human NK cells and its role in protein phosphorylation, cytokine production, and cell proliferation. J Immunol 154(3):1124-1135.
57. Liu W, Shen D, Ju L, Zhang R, Du W, Jin W et al (2022) MYBL2 promotes proliferation and metastasis of bladder cancer through transactivation of CDCA3. Oncogene 41(41):4606-4617. https://10.1038/s41388-022-02456-x
58. Li J, Chen H (2022) Actin-binding Rho activating C-terminal like (ABRACL) transcriptionally regulated by MYB proto-oncogene like 2 (MYBL2) promotes the proliferation, invasion, migration and epithelial-mesenchymal transition of breast cancer cells. Bioengineered 13(4):9019-9031. https://10.1080/21655979.2022.2056821
59. Liu M, Du Q, Mao G, Dai N, Zhang F (2022) MYB proto-oncogene like 2 promotes hepatocellular carcinoma growth and glycolysis via binding to the Optic atrophy 3 promoter and activating its

Figures

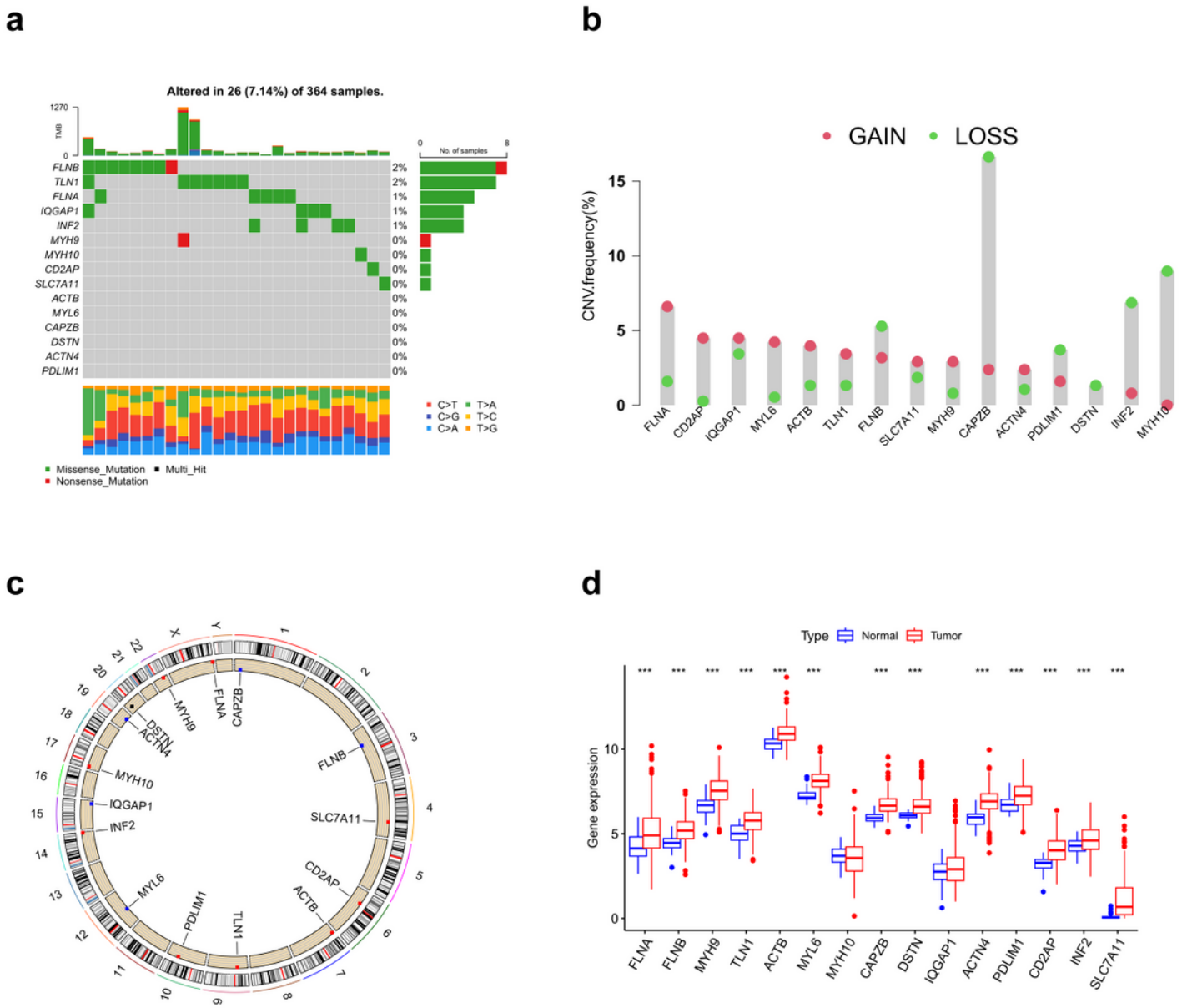

Figure 1

Genetic and transcriptional alterations of DRGs in HCC. **a**Mutation frequency of DRGs in the TCGA cohort of 364 HCC patients. **b**Copy number variation of 15 DRGs. **c** Distribution of DRGs on chromosomes. **d** Expression of 15 DRGs in HCC (TCGA) tissue versus normal. *$p < 0.05$, *$p < 0.01$, *$p < 0.001$

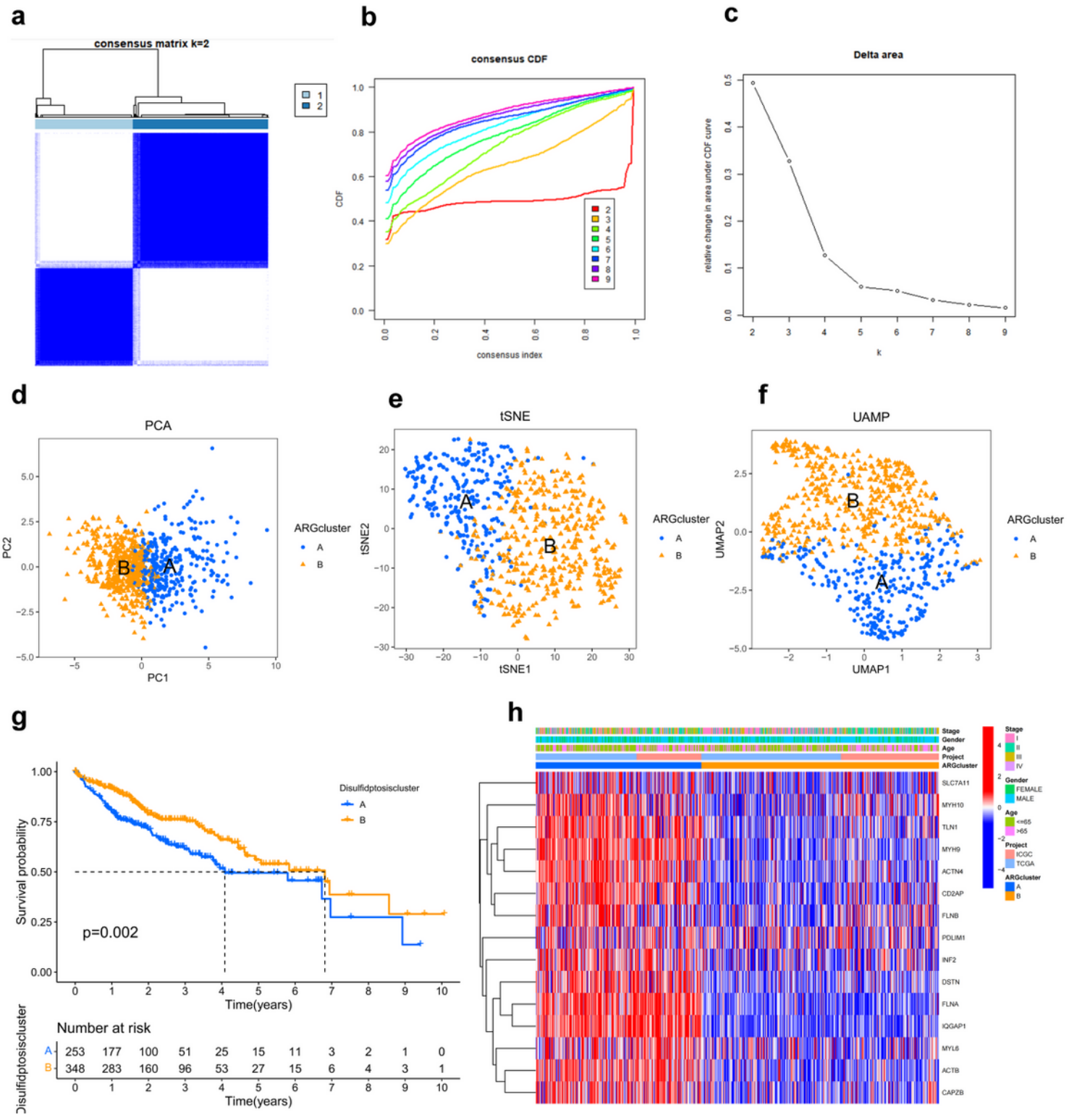

Figure 2

HCC subgroups associated with disulfidptosis. **a-c** Consensus matrix heat map of TCGA and ICGC cohort samples defining two clusters(k = 2). **d-f** PCA, tSNE, and UAMP analysis showed significant differences in transcriptome between the two subtypes. **g** Kaplan-Meier survival curves showed significant differences between the two subtypes(*P* = 0.002). **h**Heatmap of clinical characteristics between the two subtypes.

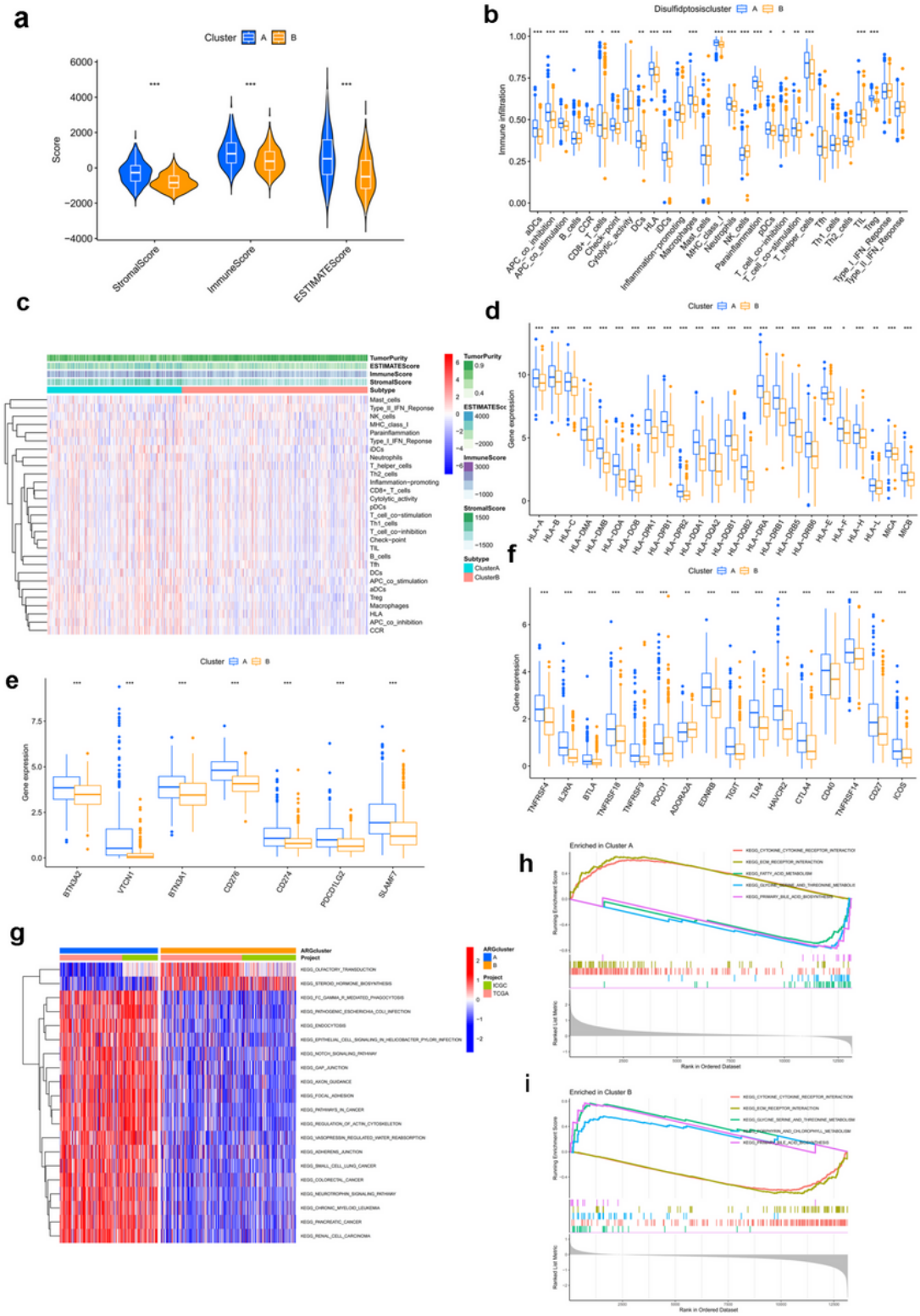

Figure 3

TME cell infiltration and biological properties of two subtypes of HCC. **a** Differences in immune score, stromal score and ESTIMATE score between subtypes. **b, c** Differences in infiltration of 29 immune cells between HCC subtypes. d Differences in expression of MHC family proteins between subtypes.**e**, **f** Expression of co-stimulatory and co-repressor molecules in 2 subtypes. **g** Biological pathways of major enrichment in 2 subtypes. **h** Pathways of enrichment of highly and lowly expressed genes in subtype A. **i**

Pathways of enrichment of highly and lowly expressed genes in subtype B. *$p < 0.05$, *$p < 0.01$, *$p < 0.001$.

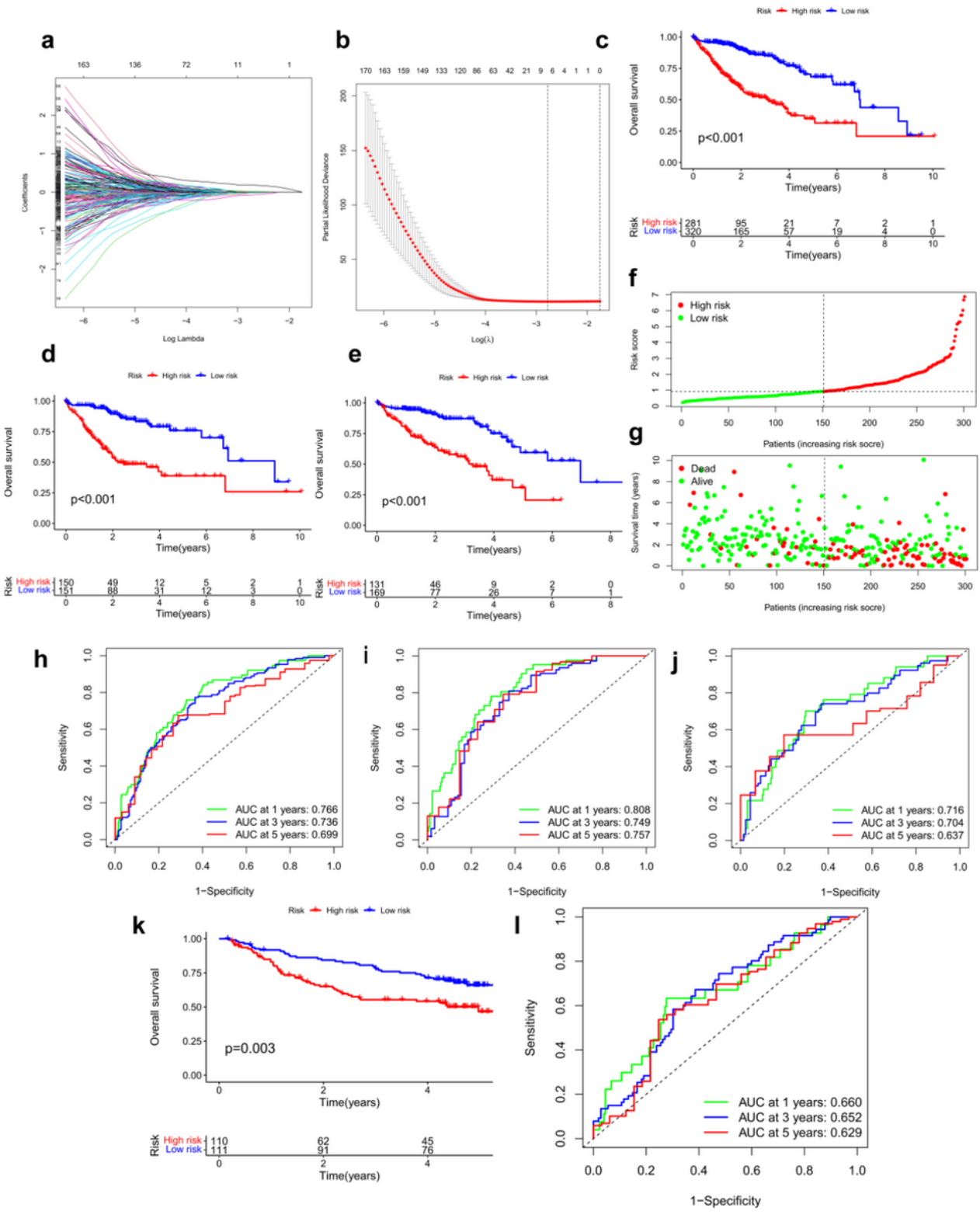

Figure 4

Construction of prognostic models for 4 genetic traits. **a, b** Lasso regression results of and cross-validation errors. **c–e** Survival curves for risk score groups in total sample, train, and test data. **f, g** Survival

status curves for risk scores. **h-j** ROC curves for total sample, train, and test data. **k** GSE14520 validation cohort risk groups for Kaplan-Meier survival curves.

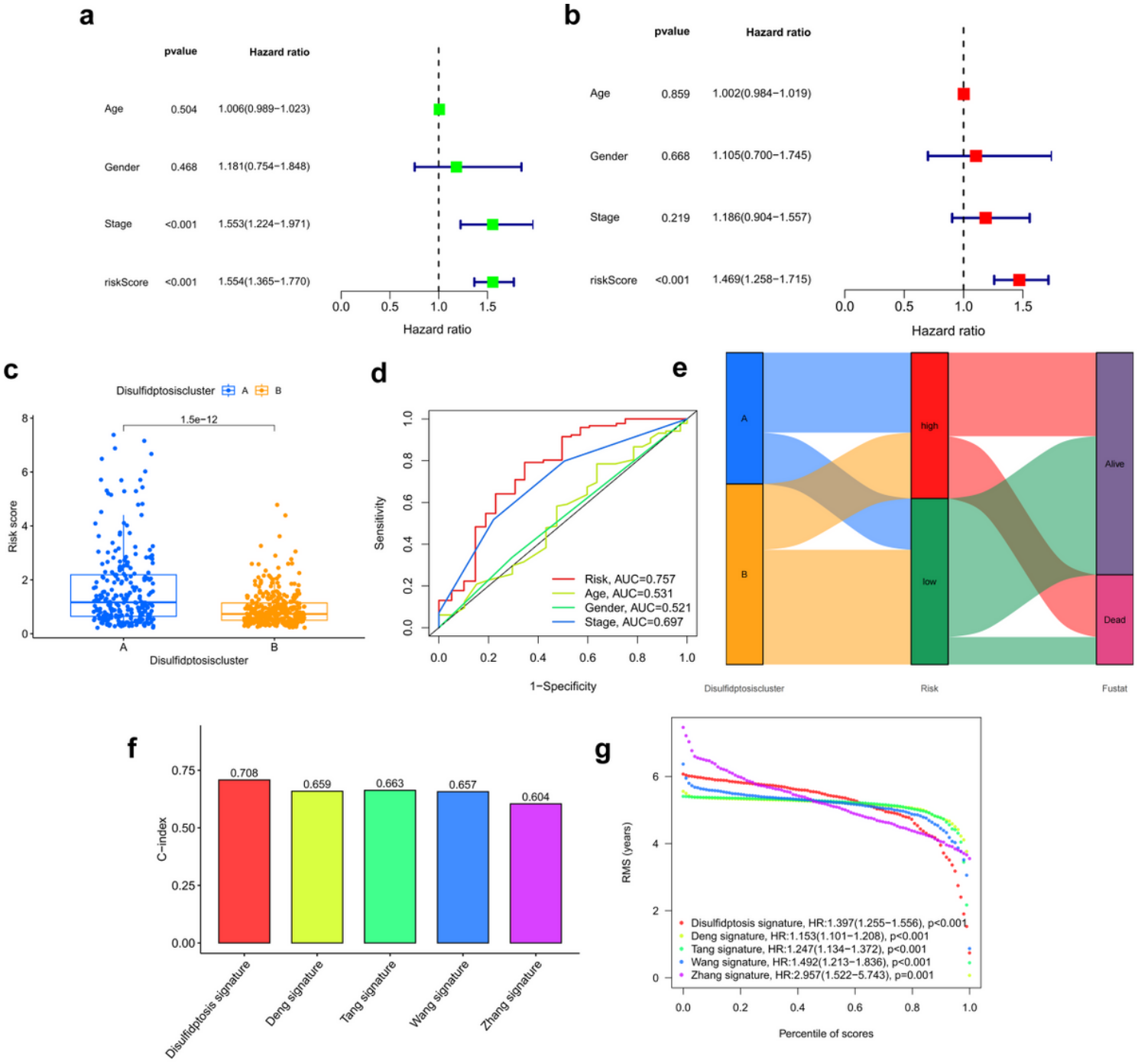

Figure 5

Survival predictive value of disulfidptosis risk model. **a** Forest plot of risk scores and clinical characteristics for univariate Cox regression analysis. **b** Forest plot of risk scores and clinical characteristics for multivariate Cox regression analysis. **c** Differences in risk scores between the two subtypes. **d** ROC curves for each clinical characteristic and risk score in the disulfidptosis model. **e** Association between disulfidptosis subtypes, disulfidptosis risk groups, and survival status. **f** Comparison

of C-index values of the disulfidptosis trait model with the four HCC trait models. **g** RMS curves of the disulfidptosis characteristic model versus the four HCC characteristic models.

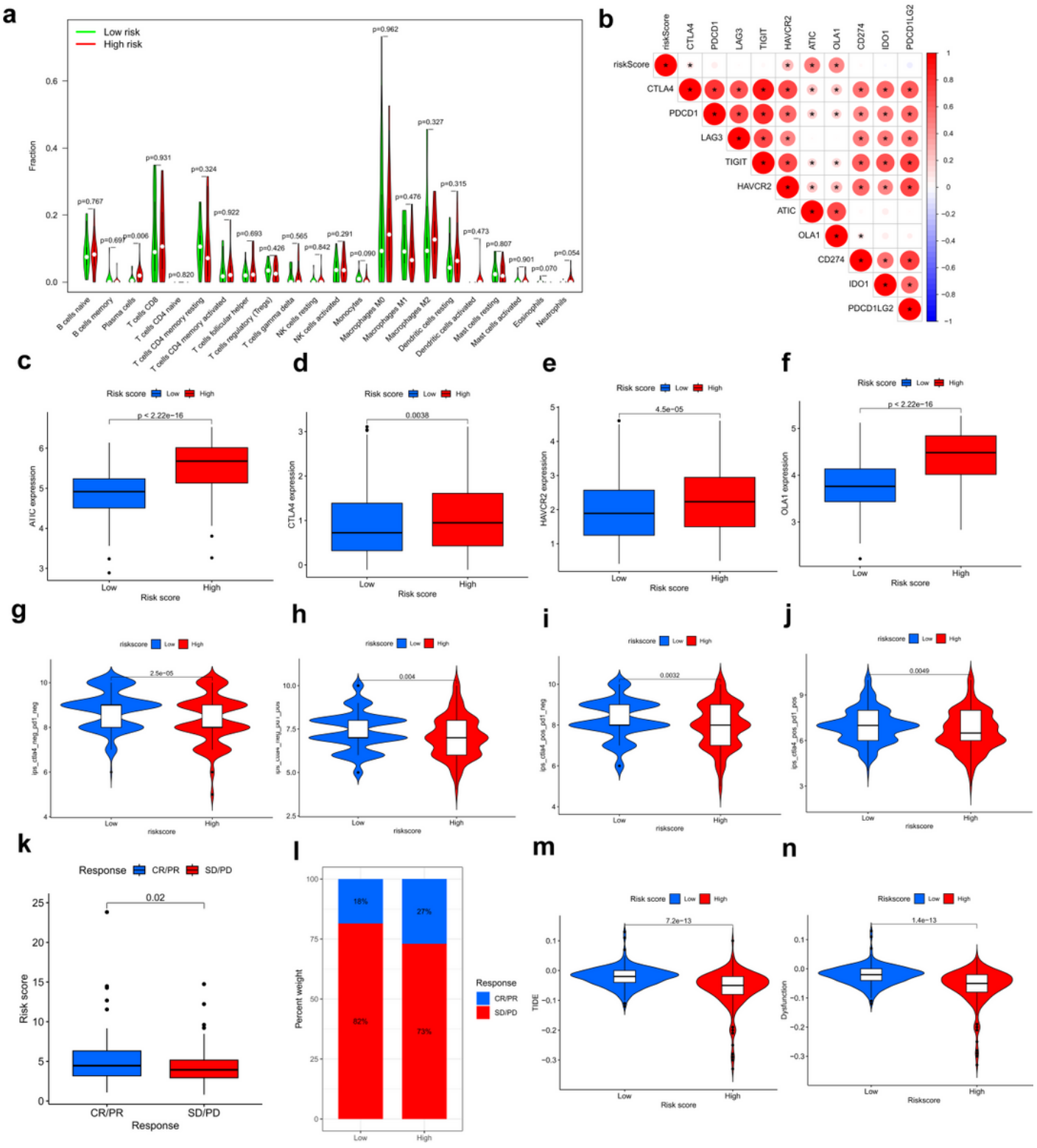

Figure 6

Tumor immune infiltration analysis with disulfidptosis risk score. **a** Infiltration abundance of 22 tumor immune cells in high and low risk groups. **b**Correlation between immune checkpoint genes and risk score.

Relative percentages of 22 immune cell subsets in 1160 samples from all LUSD cohorts. Differences in expression of AITC(**c**), CTLA4(**d**), HAVCR2(**e**),OLA1(**f**) between the two risk groups. **g-j** Differences in risk scores among the four immune check treatment groups. **k** Differences in treatment responsiveness among the risk groups in the IMvigor210 cohort. **l** Proportion of treatment response effect in different risk groups in the IMvigor210 cohort. **m** TIDE scores in different risk groups. **n** dysfunction scores in different risk groups.*$P < 0.05$.

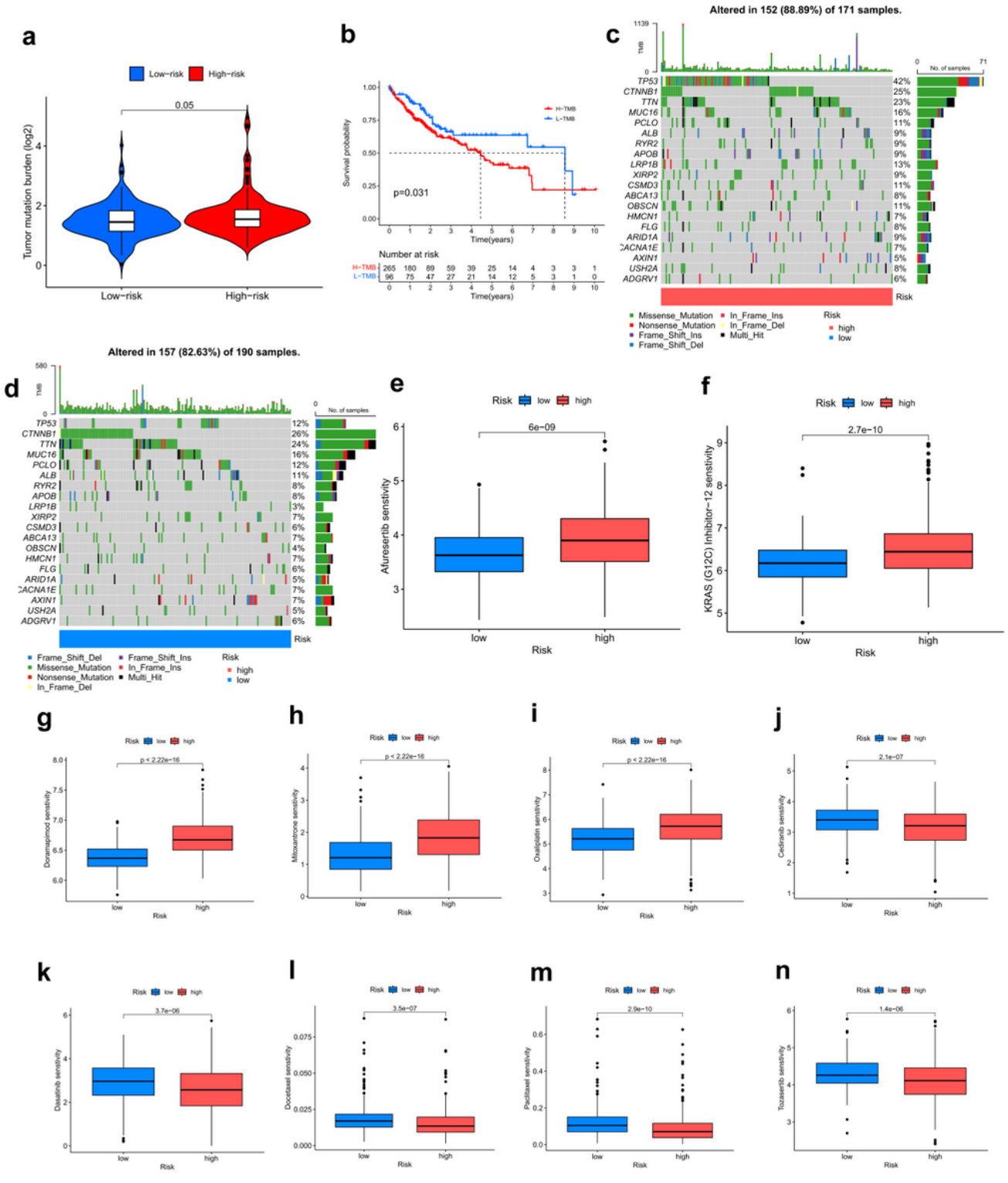

Figure 7

Mutation profile and drug sensitivity analysis of disulfidptosis risk score in HCC. **a** TMB differences between risk score groups. **b** TMB survival curves in the TCGA cohort. **c** Top 20 genes in the high risk group in terms of mutation frequency. **d** Top 20 genes in the low risk group in terms of mutation frequency. **e–n** The relationship between risk groups and drug sensitivity.

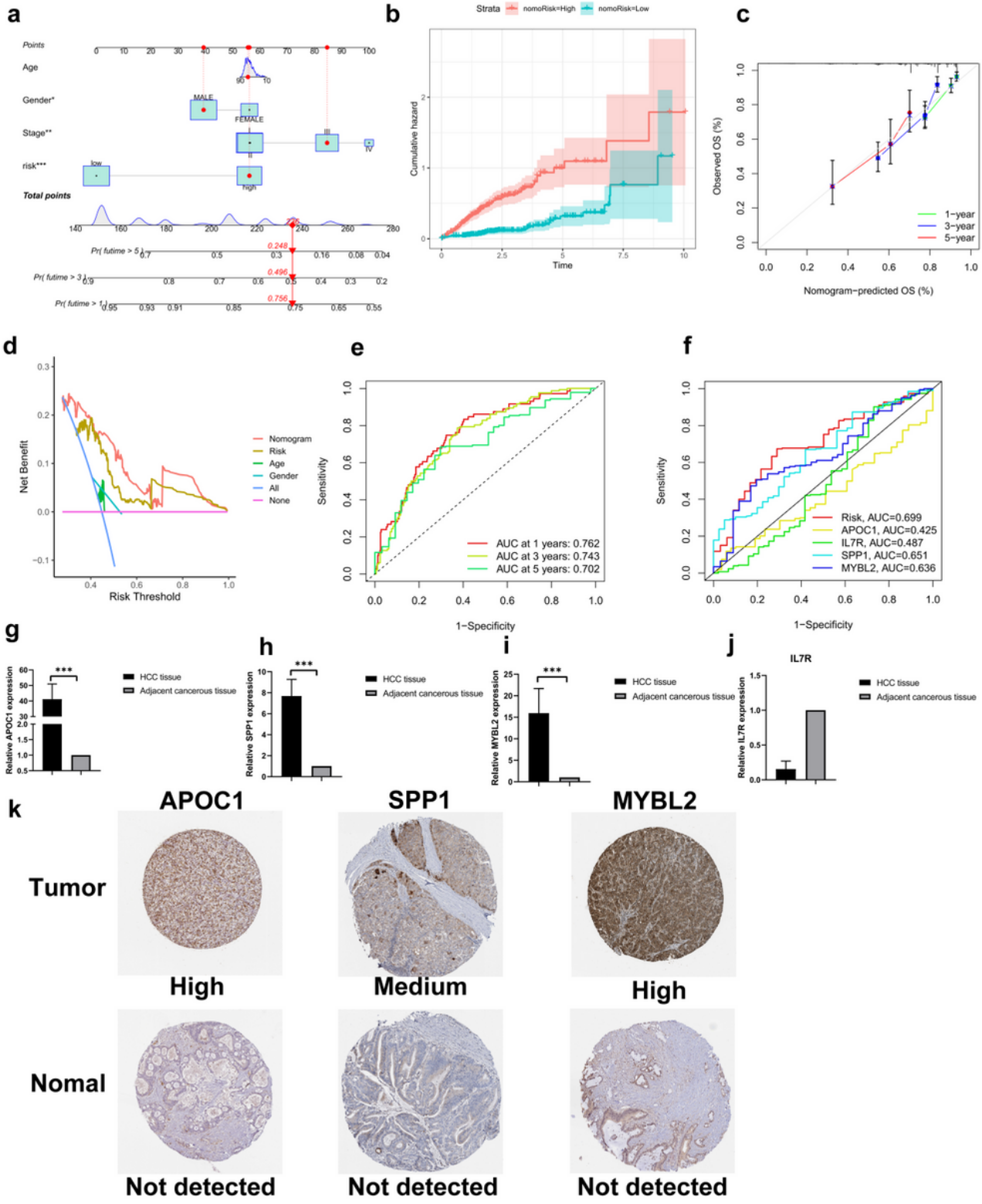

Figure 8

Nomogram plot construction and prognostic validation of the disulfidptosis model. **a** Columnar plots predicting 1, 3, and 5 year overall survival in patients with HCC. **b**Cumulative curves between nomogram risk groups. **c** Calibration curves for nomogram-predicted survival outcomes. **d** DCA curves to analyze the clinical value of each clinical feature, nomogram and risk score. **e** ROC curves for nomogram-predicted overall survival. **f** ROC curves for four risk genes in predicting HCC prognosis. The mRNA levels of APOC1(**g**), SPP1(**h**), MYBL2(**i**),IL7R(**j**) in 10 pairs of HCC and their paired adjacent normal tissues were measured by real-time fluorescence quantitative PCR. **k** Protein expression of APOC1, SPP1, MYBL2 in HCC and normal liver tissues. Data were obtained from the Human Protein Atlas(http://www.proteinatlas.org) online database.

Supplementary Files

This is a list of supplementary files associated with this preprint. Click to download.

- Supplementarymaterials.docx